J Forensic Sci, May 2006, Vol. 51, No. 3
doi:10.1111/j.1556-4029.2006.00116.x
Available online at: www.blackwell-synergy.com

TECHNICAL NOTE

Katherine Flynn,[1] *B.Sc.(Hons); Robyn O'Leary,*[1] *B.Sc.(Hons); Claude Roux,*[1] *Ph.D.; and Brian J. Reedy,*[1] *Ph.D.*

Forensic Analysis of Bicomponent Fibers Using Infrared Chemical Imaging

ABSTRACT: The application of infrared chemical imaging to the analysis of bicomponent fibers was evaluated. Eleven nominally bicomponent fibers were examined either side-on or in cross-section. In six of the 11 samples, infrared chemical imaging was able to spatially resolve two spectroscopically distinct regions when the fibers were examined side-on. As well as yielding characteristic infrared spectra of each component, the technique also provided images that clearly illustrated the side-by-side configuration of these components in the fiber. In one case it was possible to prepare and image a cross-section of the fiber, but in general the preparation of fiber cross-sections proved very difficult. In five of the 11 samples, the infrared spectra could be used to identify the overall chemical composition of the fibers, according to a published classification scheme, but the fiber components could not be spatially resolved. Difficulties that are inherent to conventional "single-point" infrared spectroscopy, such as interference fringing and sloping baselines, particularly when analyzing acrylic type fibers, were also encountered in the infrared chemical image analysis of bicomponent fibers. A number of infrared sampling techniques were investigated to overcome these problems, and recommendations for the best sampling technique are given. Chemical imaging results were compared with those obtained using conventional fiber microscopy techniques.

KEYWORDS: forensic science, chemical imaging, bicomponent fibers, infrared, FTIR, hyperspectral imaging

Fiber evidence is frequently encountered in forensic investigations and is an important class of trace evidence that can provide valuable information to support an association, for example, between two people or between a person and a crime scene. Standard forensic examinations for man-made fibers consist of microscopic techniques such as visible light, polarized light, and fluorescence microscopy, followed by microspectrophotometry. If, after that stage, two fibers are still indistinguishable, they are then examined by infrared spectroscopy, which is useful for identifying the fiber polymer type present, and then dye extraction and analysis (1).

In this paper, we examine a particular type of man-made fibers known as bicomponent fibers. Bicomponent fibers are a special class of fibers comprised of two polymers of different chemical and/or physical properties existing within the same filament. They are produced to exploit properties not existing in either polymer alone. A number of different characteristics such as strength, luster, shrinkage, dyeability, and stability of the fiber are able to be altered by the choice of chemical components and the spatial configuration of these used when manufacturing the fiber (2).

There are a number of different spatial configurations the two components may take on, with the most common examples shown in Fig. 1 (2,3). Sheath–core fibers consist of one component (core) fully surrounded by a second component (sheath). This structure is used to take advantage of the differing properties of each component; for example, the sheath material may be a more expensive material and contribute to luster and dyeability whereas the hidden core material may be chosen to reduce costs, have flame retardant properties, or add bulk and strength. Side-by-side fibers consist of two components divided lengthwise into two or more distinct regions. Side-by-side fibers are generally used as self-crimping fibers, based on the different shrinkage properties of each component (2).

The first commercial bicomponent fiber application was introduced by DuPont (Kinston, NC) in the mid-1960s. This was a side-by-side hosiery yarn made from two nylon polymers that, on retraction, formed a highly coiled elastic fiber. In the 1970s, production of various other bicomponent fibers began in Asia. The first commercial use of sheath–core-binding fibers was in carpets and upholstery fabrics. In 1998, Japan and Korea had the largest worldwide output of bicomponent fibers with a total of 90,700 metric tons produced annually. The annual production in the U.S. market was around 27,200 metric tons, with Hoechst Celanese the largest U.S. producer. The worldwide production of bicomponent fibers is only a fraction of the 25 million metric tons of man-made fiber market, but with technological advances the producers are confident of a significant growth over the next 5 years or so (4). Bicomponent fibers can be found in many different products such as clothing (e.g., sportswear developed with water-absorptive properties), carpet, upholstery/mattresses, insulating materials, and diapers (2,5).

The greater the rarity and uniqueness of a fiber among the general population, the stronger the evidence will be. Bicomponent fibers have significant forensic value due to their relative scarcity in society, and the highly distinctive chemical/spatial configurations possible. There has been a small number of forensic studies

[1]Centre for Forensic Science, University of Technology, Sydney, PO Box 123, Broadway NSW 2007, Australia.

Color versions of the figures can be found online at www.blackwell-synergy.com

Received 28 Feb. 2005; and in revised form 4 June 2005, 30 Oct. 2005; accepted 5 Nov. 2005; published 5 April 2006.

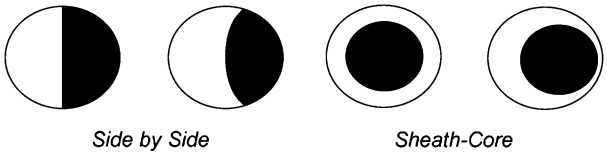

FIG. 1—*Common configurations for bicomponent fibers.*

conducted on bicomponent fibers. The first study by Grieve et al. (6) investigated a number of different techniques for recognizing, characterizing, and comparing bicomponent acrylic fibers. The techniques examined included brightfield and polarized light microscopy, cross-sectioning, IR spectroscopy, and scanning electron microscopy (SEM). At the time of their study, it was reported that commercially produced acrylic bicomponent fibers seemed to be exclusively of the side-by-side variety, and hence it was this configuration investigated in their work. Grieve et al. recognized the need for further analytical techniques to be investigated owing to the increased number of bicomponent fibers encountered in casework, and noted that in regular testing, the bicomponent nature of these fibers was often not being revealed, and hence their evidential value was not being completely recognized and exploited.

Grieve et al. found that normal microscopic examination using brightfield and polarized light microscopy was not always effective in recognizing bicomponent fibers. Only in instances where there was a difference in the delusterant concentrations between the two components of the fibers was it revealed that the sample was bicomponent using brightfield microscopy. Similarly, under polarized light, a slight birefringence difference between the two halves was the only indication that the fibers may contain slightly different polymers. However, many of the bicomponent fibers examined did not show variable birefringence. Cross-sectional analysis with examination by light microscopy and SEM were also found to be largely ineffective in recognizing fibers as being bicomponent. SEM only gave a clear indication that one of the nine fibers studied was bicomponent, and cross-sectional analysis was only useful where there was a difference either in delusterant composition or colour variation between the two components.

Infrared spectroscopy was shown to be a more successful technique in recognizing and characterizing bicomponent fibers. Given that all the fibers studied were of the side-by-side variety, FTIR microscopy could be used to collect spectra of each half of the fiber to reveal the identity of the two polymers. A drawback to this approach in forensic casework, however, is that the structure of the bicomponent fiber might not be known before analysis.

Grieve et al. concluded that the majority of acrylic bicomponent fibers encountered in their casework were recognized only if they had varying delusterant concentration, or consisted of different-colored components. For example, the techniques evaluated by Grieve et al. failed to identify bicomponent fibers in an evidential garment known to contain Monsanto (Greenwood, SC) bicomponent acrylic fibers. Grieve et al. also conceded that unless a fiber's bicomponent structure is microscopically obvious under transmitted light, bicomponent acrylic fibers may go unnoticed; no remedy was found for this in their studies.

Following this research, Tungol et al. (7) examined infrared spectroscopy for the analysis of sheath–core bicomponent fibers. They found through the use of apertures that, for flattened sheath–core bicomponent fibers, an infrared spectrum of the sheath component alone could be obtained at the edge of the sample, and a combined sheath–core spectrum could be obtained from the middle of the fiber sample. Through the use of spectral subtraction, a spectrum of the sheath material could be obtained.

In a later study carried out by Cho et al. (8), both attenuated total reflection (ATR) and transmission infrared microspectroscopy were used for the qualitative analysis of bicomponent fibers. In this study, only sheath–core bicomponent fibers were examined. Cho et al. demonstrated that with the use of both ATR and transmission techniques, spectral information could be obtained for both the sheath and core components of the fiber. As ATR is a surface-preferenced technique, it should in theory allow for the spectrum of the sheath component only to be obtained. Transmission analysis yields a combined spectrum of both the core and sheath components. Through spectral subtraction of the two spectra, they were able to obtain a spectrum mainly corresponding to the core material. Problems with this approach include the possibility of not obtaining a completely pure spectrum of each component, and also shifts in peak frequency and intensity values can occur with ATR analysis relative to transmission analysis. These shifts in frequency values may be problematic when obtaining the core spectrum, which involves subtracting an ATR spectrum (sheath) from the transmission spectrum (core and sheath), and could potentially lead to inaccurate results in identifying the core polymer type (1).

One major drawback with the infrared techniques described above is that the spatial configuration of the fibers, i.e., whether they are side-by-side or sheath–core, needs to be known before infrared analysis. This information is unlikely to be available in a forensic case scenario unless it is microscopically obvious. Ideally, a complete forensic analysis of bicomponent fibers should reveal both the chemical composition and the spatial distribution of the components present.

Infrared chemical imaging is a technique that may enable the complete characterization of bicomponent fibers, as it allows for spatially resolved chemical data to be collected from a sample. The Digilab "Stingray"® (Digilab, Randolph, MA) infrared chemical imaging system used in this study has a 64×64 pixel mercury cadmium telluride (MCT) focal plane array (FPA) detector. Using this detector, 4096 infrared spectra can be obtained simultaneously in the form of an image, with one spectrum recorded for each pixel. This is in contrast with conventional infrared microscopy, where only one spectrum can be collected at a time. The image data collected can be thought of as a three-dimensional datacube, which contains vertical and horizontal spatial dimensions, and a spectral frequency dimension. (9,10). There are a number of different ways that this data can be visualized, including selecting a particular point on the sample and obtaining the infrared spectrum at that location, or forming images ("false color maps") based on the spectral intensity at particular frequencies. In the latter case, the data can be viewed as a series of images, with one image at each wavenumber resolution unit.

A number of parameters can be used to form chemical images including peak height, peak area, or ratios of areas or heights at different frequencies of interest. A false color map is formed by assigning an arbitrary color to each pixel according to the intensity of the particular parameter selected. Most commonly, a scale from high intensity red to low intensity blue is used (the scale used throughout this research); however, other options such as grayscale are available. By imaging at frequencies corresponding to the vibrations of chemical functional groups, the spatial distribution of different chemical components in the sample can be seen. More detailed information on the theory of infrared chemical imaging can be found elsewhere (9,11).

In this paper, infrared chemical imaging is investigated as a more suitable and informative technique to analyze bicomponent fibers than conventional infrared spectroscopy. Its main advantage is its ability to simultaneously collect hundreds to thousands of infrared spectra from across the whole sample to potentially reveal any inhomogeneity present in the sample, such as a second polymer component, without the need for any prior knowledge on the sample. Other conventional techniques (brightfield—polarized—fluorescence microscopy, SEM) were also applied in order to compare the value of infrared chemical imaging to more established techniques for the forensic examination of fibers.

Materials and Methods

Sample Details

Eleven bicomponent fiber samples, listed in Table 1, were obtained from two reference libraries, the Microtrace "Forensic Fiber Reference Collection" (2001, USA) and the CTS Reference Collection of Synthetic Fibers (1987, USA).

Conventional Testing

Microscopic Techniques—Fiber samples were mounted using a 50% glycerine/water mixture and examined using brightfield, polarized and fluorescence microscopy. A Leica DMR Fiber Comparison Microscope (Leica, Nussloch, Germany) was used to examine the fibers at $\times$ 200 or $\times$ 500 magnification. Photographs were taken using a Leica MPS52 camera.

Environmental Scanning Electron Microscopy (ESEM)—The cross-sections of each fiber sample, embedded in either Serifix or UV-curable resin (see below), were examined using a FEI XL30 ESEM with a gaseous secondary detector (GSE) at magnifications ranging from $\times$ 1000 to $\times$ 5000.

Infrared Chemical Imaging

Infrared chemical imaging of the bicomponent fibers was carried out using a Digilab Stingray system, comprised of an FTS7000 FTIR spectrometer, coupled to a UMA600 infrared microscope fitted with a Lancer 64 $\times$ 64 FPA detector. Images and spectra were collected and processed with Digilab Win IR Pro software. All samples were imaged using the "normal field of view," in which each individual image tile is *c.* 350 $\times$ 350 μm in size. The spectral range collected was 900–4000 cm^{-1}, with the lower value determined by the limit of the FPA detector. In a typical data set, the spatial resolution varies depending upon the wavelength chosen to form the image. At best, this will be *c.* 5.5 μm at higher wavenumber values, determined by the detector (pixel) size, and at worst, it will be *c.* 15 μm, restricted by the wavelengths of light involved at the low wavenumber end of the spectrum.

A number of different infrared sampling methods were used to analyze each of the bicomponent fiber samples, including normal transmission analysis and two micro-sampling techniques, using a diamond anvil miniature cell (DAC) (High Pressure Diamond Optics Inc., Tucson, AZ) or a germanium ATR microscope objective (Harrick Scientific SplitPea, Ossining, NY).

Transmission—For transmission analysis, a single fiber was taped across a window cut out of acetate frames (EXP photocopier transparency sheets, Corporate Express, Sydney, Australia), and then flattened using a hand-held metallic roller (Kevley Technologies, Chesterland, OH). The hand-held metallic roller surface was first "roughened" using silicon carbide paper, to avoid producing a thin layer with a smooth surface, which can lead to interference fringing (1). When analyzing in transmission mode, absorbance spectra were collected at 8 cm^{-1} resolution, using 256 co-added scans. Background images were collected adjacent to the sample through air.

Diamond Anvil Cell (DAC) Accessory—A single fiber was placed between the two diamond faces and flattened to a suitable thickness for infrared transmission analysis. A slight rocking of the diamond cells was employed when flattening the fibers to avoid producing a thin flat film, and hence minimize interference fringing. The top half of the diamond anvil cell was then removed, and infrared analysis conducted through one half of the cell only, also to reduce interference fringing (1). Absorbance spectra were collected at 8 cm^{-1} resolution using 256 co-added scans. Background images were collected from vacant areas of one diamond face. Some problems were encountered with the analysis of the acrylic bicomponent fibers, with sloping baselines and interference fringing appearing in the infrared spectra obtained. In an attempt to overcome these problems, a drop of paraffin oil was occasionally added to the diamond anvil cell (see Results and Discussion).

ATR Microscope Accessory—A single fiber was taped straight at both ends to a microscope slide and analyzed using a germanium hemispherical ATR crystal. To obtain infrared chemical images, the ATR crystal was placed in contact with the fiber sample and a contact alert system (SpectraTech, Stamford, CT) used to monitor the pressure applied. For ATR analysis, it was necessary to collect a higher number of co-added scans and, for absorbance spectra collected at 8 cm^{-1} resolution, at least 1024 co-added scans were required.

TABLE 1—*Polymer compositions of fiber samples determined by the authors using published classification schemes and the microtrace fiber reference collection.*

Fiber	Manufacturer	Polymer Composition	Spatial Characterization
Cashmilon G4K	Asahi Chemical Co.	PAN-MA-AA/PAN-MA	Side-by-side
Acrilan B57	Monsanto	PAN/VA	No
Acrilan B94	Monsanto	PAN/VA	No
Monsanto X-24	Monsanto	PAN/VA based (with minor spectral variations in range 1000–1300 cm^{-1} that concur with Grieve's spectrum 1995)	No
Monvelle	Monsanto	PA/PU	Side-by-side
Velicren bicomponent	Snia	PAN/MA/Sulfonate+DMF	No
Beslon F040	Toho Rayon	PAN-MA-AA/PAN-MA	Side-by-side
Orlon 21	DuPont	PAN/PAN-SS	Side-by-side
Cantrece	DuPont	Nylon 6,6/Unknown polyamide component	Side-by-side
Creslan 68	American Cyanamid Co.	PAN/MMA (without DMF solvent)	No
Dralon K	Bayer	PAN/MA/Sulfonate+DMF	Side-by-side

PAN, pure acrylonitrile; MA, methylacrylate; AA, acrylamide; VA, vinyl acetate; DMF, dimethylformamide; PA, polyamide; PU, polyurethane; SS, styrene sulfonate; MMA, methylmethacrylate.

Cross-Sectional Analysis—Cross-sectional analysis was also attempted for the fibers. The fibers were first taped across a window in acetate sheeting, as described previously, to assist with positioning for sectioning and also to prevent the fibers from crimping (12). They were then set in a variety of resins including Serifix (Struers, Copenhagen, Denmark), Spurrs (ProSciTech, Thuringowa, Australia) and a UV curable resin (Loctite, Munich, Germany). Because of difficulties locating the colorless fiber cross-sections in the colorless resins, methyl violet 6B indicator (Searle Diagnostic, High Wycombe, U.K.) was used to dye the resins purple. Sections of 5–10 μm thickness were microtomed using a Leica RM2165 motorized microtome. The fiber cross-sections were then placed on potassium bromide (KBr) plates and imaged in transmission mode as described previously. Background images were obtained from vacant areas of the KBr plates.

Results and Discussion

Conventional Testing

Varied results were obtained using conventional methods of analysis. None of the fibers exhibited any fluorescence and therefore fluorescence microscopy gave no indication as to whether or not the fiber samples were bicomponent.

Brightfield microscopy was found to be slightly more successful and did allow for a few of the fibers to be identified as bicomponent. The clearest indication was seen for Orlon 21 (DuPont) in which the two components could be easily distinguished due to the difference in delusterant concentration (Fig. 2). One half of the fiber appears transparent, while the other side contains brown speckles, due to the delusterant. Brightfield microscopy clearly demonstrates that this bicomponent fiber is of a side-by-side configuration. A slight difference in delusterant concentration could also be seen for Monsanto X-24, revealing its side-by-side configuration. For the remainder of the fiber samples, there was no clear indication that the fibers were bicomponent. In some of the samples, namely Monvelle (Monsanto), Velicren bicomponent (Snia, Milan, Italy) and Dralon K (Bayer, Dormagen, Germany), a faint division line could be seen down the middle of the fiber samples, indicating that the fibers could be side-by-side bicomponents (Fig. 3). In six of the 11 samples examined, there was no indication using brightfield microscopy that these fibers were indeed bicomponent fiber samples.

FIG. 2—*Brightfield microscopy visible light image of Orlon 21 (DuPont) at × 200 magnification demonstrating difference in delusterant concentration.*

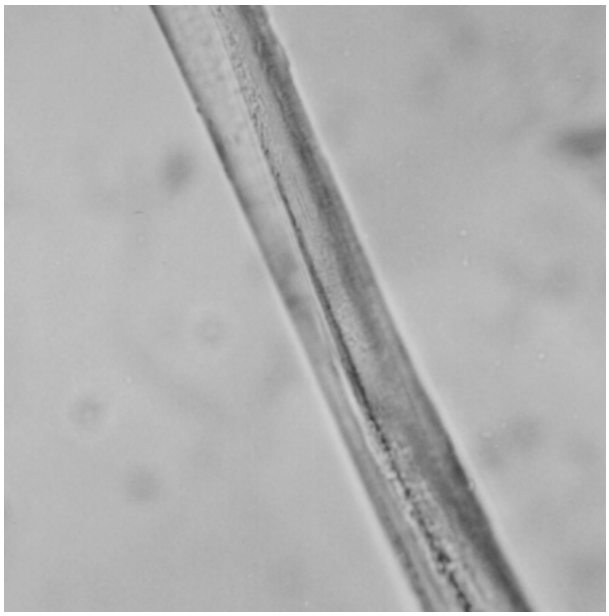

FIG. 3—*Brightfield microscopy visible light image of Monvelle (Monsanto) at × 200 magnification, showing faint division line visible down middle of sample.*

Polarized microscopy was not very successful in revealing the fibers as bicomponent. A slight difference in birefringence could be seen for Acrilan B94, with one half of the fiber appearing a paler aqua blue than the other. As with brightfield microscopy, a very faint division line could be seen down the middle of three samples, Velicren bicomponent (Snia), Orlon 21 (DuPont), and Dralon K (Bayer). For seven samples, there was no indication that these samples were bicomponent fibers.

Environmental SEM was very successful in revealing Monvelle (Monsanto) as a side-by-side bicomponent fiber (Fig. 4). The two components could be clearly distinguished using this technique, and was the most successful result of all fibers tested. For the remaining samples, there was either only a very slight division line that could occasionally be seen in the cross-section and that was not always visible across the whole diameter of the fiber, or there was no indication at all that the fibers were bicomponent.

Infrared Chemical Imaging

A number of different sampling methods were used to analyze the bicomponent fiber samples. It was found that normal transmission analysis and the use of a diamond anvil cell produced good quality infrared spectra for the nylon-type fibers, Monvelle (Monsanto) and Cantrece (DuPont); however, problems were encountered when analyzing the acrylic bicomponent fibers. Interference fringing, which appears as a sinusoidal wave in the baseline, was seen in many of the spectra obtained, along with sloping baselines. This is not uncommon in the single-point infrared analysis of acrylic fibers in general. There are a number of

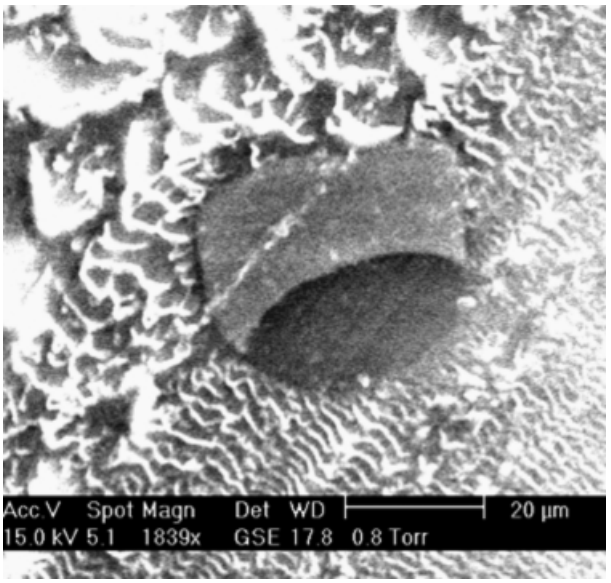

FIG. 4—*Cross-section image of Monvelle (Monsanto) obtained using environmental scanning electron microscopy.*

reasons why interference fringing can occur, such as if fiber samples are flattened on a smooth surface to produce a thin film (due to internal reflections of the infrared beam within the sample), and they can also occur when using a diamond anvil cell accessory (due to multiple reflections occurring at the diamond faces) (1). To overcome these problems, the fiber samples were flattened using a roughened metallic hand-roller for transmission analysis, to avoid obtaining a thin smooth sample, and infrared spectra were acquired through only one diamond face (as is the normal practice), to reduce reflections occurring between the diamond faces. Several other attempts were made to overcome this interference fringing including: (i) the addition of paraffin oil to the diamond anvil cell to remove air gaps and thus reduce refractive index differences (1,13); and (ii) the use of an ATR microscope accessory.

The first option, which involved the addition of a drop of paraffin oil to the diamond anvil cell, did reduce the amount of interference fringing seen in the infrared spectra. This is due to the refractive index of paraffin being higher than that of air. The large difference in refractive index between diamond (2.42) and air (1.003) (or the sample in question) contributes to interference fringing. The addition of paraffin oil (1.48) reduces the overall difference in refractive indices, which in turn reduces reflection at the diamond interface, and this leads to less interference fringing (1,13). Paraffin oil was chosen because, although it will contribute to the infrared spectra of the fiber sample, paraffin has very few infrared bands and therefore its contribution can be easily monitored and, if desired, spectrally subtracted before library searching for fiber identification. Another option would be the use of KBr powder, which is not quite as convenient as paraffin to use in this way, but has the advantage of having no infrared peaks.

The second option, using a germanium ATR accessory, was able to produce very good quality infrared spectra without interference fringing. There are, however, a number of drawbacks when using ATR imaging, including that a much higher number of co-added scans were required to obtain an acceptable signal-to-noise ratio. At least 1024 scans are recommended, which takes a total time of 25 min (at 8 cm^{-1} resolution), compared with 5–6 min for the 256 scans required to analyze the fibers in transmission. Another difference between ATR imaging and the transmission methods tested is the image size possible. With ATR imaging, due to the high refractive index of the ATR crystal, a field of view of only 90 µm × 90 µm is obtained (14,15). For the analysis of many of the bicomponent fiber samples, which ranged from 20 µm to around 80 µm in diameter, this image size is still satisfactory. It was found, however, that for all of the bicomponent samples tested in this research, ATR imaging was only able to image one component, and therefore did not reveal any of the fibers as being bicomponent. This could be due to ATR imaging being a surface-preferenced technique, which means it would most likely not detect a sheath–core configuration, as only the sheath material would be imaged by the ATR crystal. Unfortunately, the spatial configurations (i.e. sheath–core or side-by-side) of the samples analyzed in this research were generally unknown, with the fiber reference libraries identifying these samples only as being bicomponent. From previous studies and results obtained from this study, some of the fiber samples were known to be side-by-side bicomponent fibers, and theoretically should have been identified as such by ATR imaging (6). It may be that, by chance, the ATR crystal was only making optical contact with one component of the side-by-side fibers. For this reason, multiple samples were prepared and many repeat tests were conducted; however, ATR imaging still failed to detect any second component present in the known side-by-side bicomponent fiber samples. For the reasons discussed previously, infrared analysis using either normal transmission mode or the use of a diamond anvil cell is recommended as the most suitable and practical sampling methods. If major problems are encountered with interference fringing and sloping baselines, then ATR imaging may assist in obtaining better quality spectra of at least one component.

Overall, infrared chemical imaging had varied success in identifying the presence of two chemically distinct regions in each bicomponent fiber sample. Published classification schemes, including Grieve's (1995) acrylic fiber identification key, were used in conjunction with other references (Grieve, 1988; Kirkbride & Tungol 1999) to identify the chemical compositions of the fibers (1,6,16). In six of the 11 samples examined, two side-by-side components could be clearly distinguished and in most cases these components could be characterized (see Table 1). An example of one of these is the Monvelle (Monsanto) fiber, which is identified in the Microtrace Fiber Reference Collection as containing polyamide and polyurethane components. Figure 3 shows the visible light image of the sample, in which only a faint division line can be seen, possibly indicating that the sample is a bicomponent fiber. However, infrared chemical images, formed by imaging the integrated spectral intensity under peaks centered near 1641 cm^{-1} (amide I in polyamide) and 1735 cm^{-1} (carbonyl stretch in polyurethane), clearly reveal not only that this sample is bicomponent, but also show its spatial configuration to be that of a side-by-side bicomponent fiber (Figs. 5*a* and 5*b*). The two components are clearly distinguished, and the infrared spectra for each component can be easily obtained, simply by clicking on a pixel from each side. The infrared spectra for each component are shown in Figs. 5*c* and 5*d*, where the peaks used to form the corresponding chemical images are highlighted. Figures 2, 5–10 are presented in color in the Web version of this article.

Two other samples that were revealed to be of side-by-side configuration were Beslon F040 (Toho Rayon, Tokyo, Japan) and Cashmilon G4K (Asahi Chemical Co., Osaka, Japan), both of which have previously been identified by the Microtrace Fiber Reference Collection as containing PAN-MA-AA/PAN-MA (see Table 1 for abbreviations). Acrylamide can be added to one side of a bicomponent fiber to produce a different shrinkage potential in

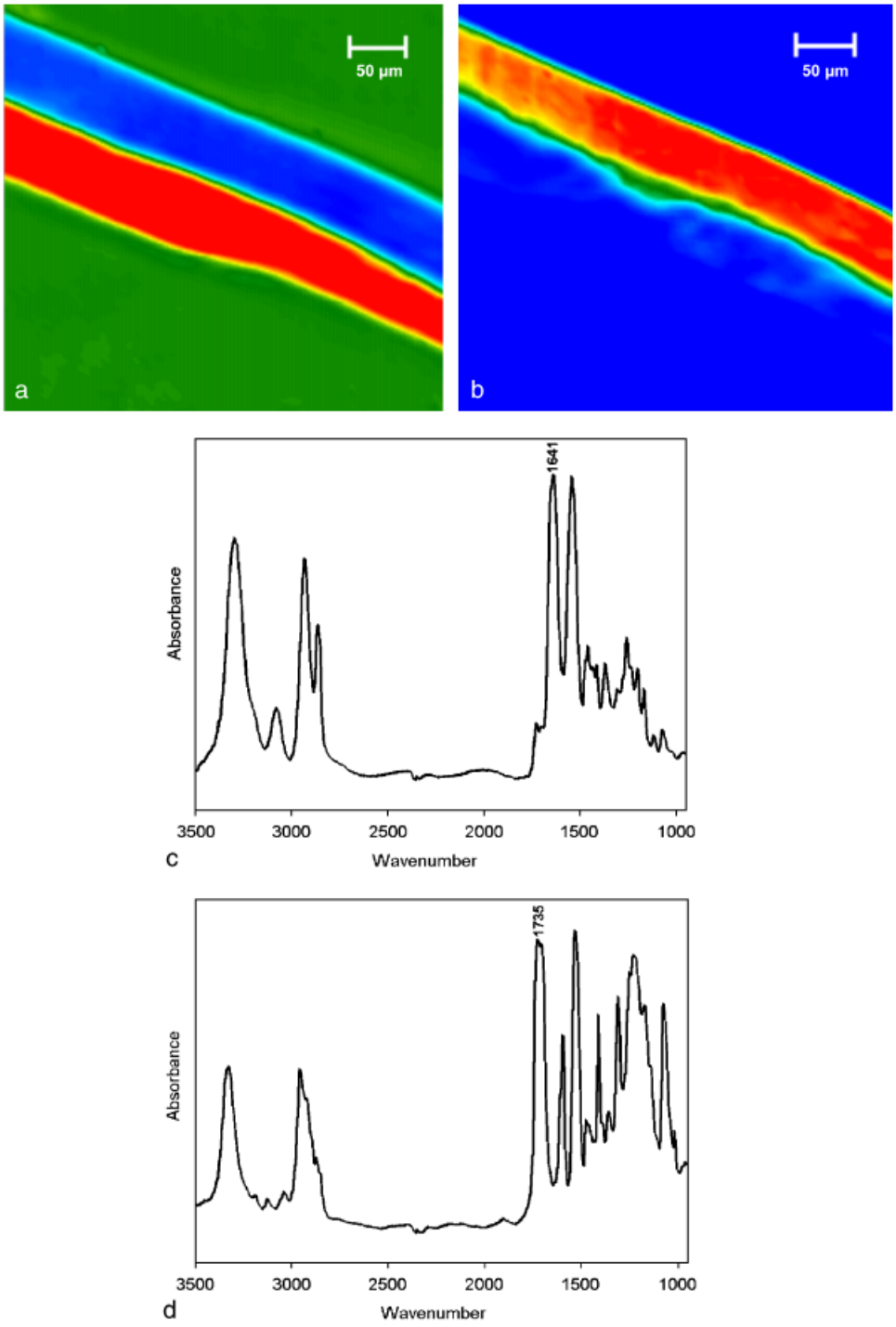

FIG. 5—*Infrared chemical image of Monvelle (Monsanto) formed by imaging at (a) 1641 cm^{-1} and (b) 1735 cm^{-1}. Infrared spectrum of (c) bottom component, identified as nylon, and (d) top component, identified as polyurethane, from Monvelle (Monsanto).*

that side, which generates a permanent crimp in the fiber (16). It was possible to distinguish the two components in these fibers by imaging on the characteristic amide I (C = O) peak for acrylamide at 1684 cm^{-1} (integrated intensities under peaks are used for all images in this paper). As similar images and spectra were obtained for these fiber samples, the results for Beslon F040 only are shown here. The first infrared chemical image shown, Fig. 6*a*, was formed by imaging on a peak that is common to both acrylic components, the nitrile (C ≡ N) functional group at 2244 cm^{-1}. As this peak is common to both components, the entire width of the fiber is highlighted (i.e., both components can be seen and appear the same). However, by imaging on an infrared peak present in only one of the components (1684 cm^{-1} due to acrylamide), only that component is highlighted (Fig. 6*b*). As noted previously, it is easy to obtain the infrared spectrum from each component simply by clicking on a pixel from each component (Fig. 6*c*).

As can be seen with the above examples, there were two possible ways the chemical images could be formed to highlight the spatial configuration of the components. With Monvelle (Monsanto) the two components could be clearly imaged independently as there were infrared bands present in each component that were characteristic of only that component. However, as could be seen

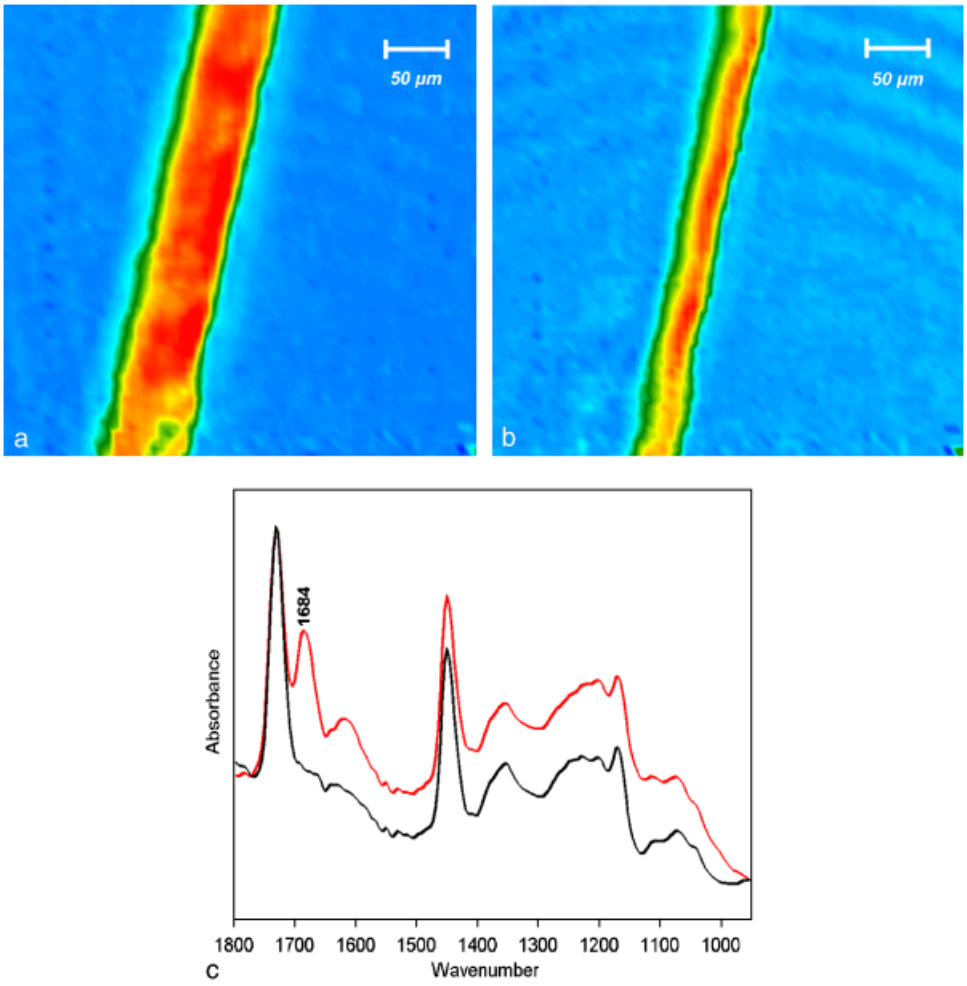

FIG. 6—*Infrared chemical image of Beslon F040 (Toho Rayon) formed by imaging using the peak area at (a) 2244 cm^{-1} and (b) 1684 cm^{-1}. c) Infrared spectra of the two components in Beslon F040 (Toho Rayon). Spectra have been truncated for Figs. 6–9 to allow minor differences to be seen more clearly.*

for Beslon F040, only one side of the fiber contains a polymer (acrylamide in this case) that enables it to be imaged independently. In these cases, the spatial configuration is revealed by imaging the entire fiber width, and comparing this with the image of the side containing the distinctive component.

The remaining three samples for which two regions could be distinguished, i.e., Orlon 21 (DuPont), Cantrece (DuPont), and Dralon K (Bayer), gave images that were similar to those already shown. For Orlon 21 (DuPont), which has previously been identified as containing PAN/PAN-SS, the entire width of the fiber is highlighted by imaging on the common acrylic peak at 2244 cm^{-1} (Fig. 7*a*). The component containing styrene sulfonate was highlighted by imaging on either one of the characteristic doublet peaks at 1011 and 1036 cm^{-1}, which have been assigned to, respectively, in-plane bending of the benzene ring and a symmetric vibration of the SO_3^- group (Fig. 7*b*) (17). Another peak that could be used to image the PAN-SS component was a shoulder at 1191 cm^{-1} (antisymmetric SO_3^- vibration) (17). The infrared spectra of the two components are shown in Fig. 7*c*, in which the peaks that can be used to image the PAN-SS component are indicated. Similar images were obtained for Dralon K, which was found to contain PAN/MA/Sulfonate+DMF, according to Grieve's classification scheme (16). The entire width of the fiber was highlighted by imaging on the acrylic peak (2244 cm^{-1}) as shown in Fig. 8*a*, however, it was found that one side appeared to contain a higher amount of methylacrylate, due to the increased peak intensity at 1730 cm^{-1} (the carbonyl group from the ester) (16). By imaging on this peak, only half the fiber width is highlighted (Fig. 8*b*). The infrared spectra of the two components are shown in Fig. 8*c*, where the increased peak intensity at 1730 cm^{-1} is indicated, and also minor differences can be seen between 1250 and 1170 cm^{-1}. It has been reported that the amount of methylacrylate is significant as it influences the shrinking capacity of the fiber, therefore the addition of extra methylacrylate to only one side of the bicomponent fiber can generate a differential shrinkage potential, leading to a permanent crimp in the fiber (16). Images similar to those shown for Monvelle (Monsanto) were obtained for the Cantrece (DuPont) fiber sample. Cantrece (DuPont) contains nylon 6,6 and another unknown polyamide component. The exact identification of the other component was not possible; however, minor but reproducible spectral differences between the components could be used to image each side-by-side component, with one side containing a shoulder at 1246 cm^{-1} (Fig. 9*a*), and the other side increased intensity of a peak at 1201 cm^{-1} (Fig. 9*b*). Figure 9*c* shows the infrared spectra and the characteristic infrared peaks used to form the chemical images that reveal the side-by-side configurations.

In some of these successful cases, some attempts failed to spatially characterize the two distinct regions, i.e., only one (apparently combined) infrared spectrum could be seen throughout the

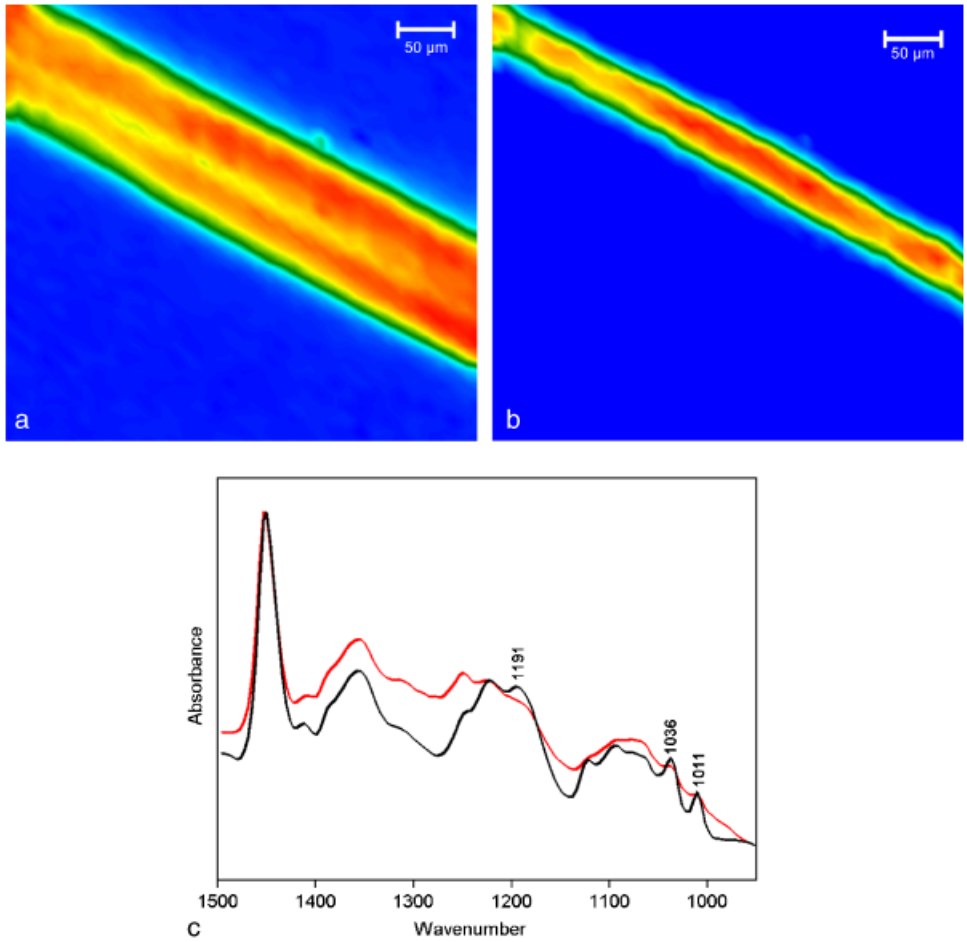

FIG. 7—*Infrared chemical image of Orlon 21 (DuPont) formed by imaging using the peak area at (a) 2244 cm^{-1} and (b) 1036 cm^{-1}. (c) Infrared spectra of the two components in Orlon 21 (DuPont).*

entire width of the fiber. A possible reason for this is that one component may have been flattened over the other, and hence the infrared beam passed through the two components at the same time, producing a mixed spectrum of the two components. For this reason, multiple samples were prepared and analyzed. This scenario may lead to potential problems in actual casework, where there may only be limited sample available to analyze. Where possible, it is recommended that repeat preparations (i.e., flattening of the fiber) and analyses of samples is undertaken, to ensure that the extra spatial information is not lost due to the way that the fiber is flattened.

For the rest of the five samples, infrared chemical imaging failed to spatially recognize more than one distinct region being present in each sample. This may have been due to the spectral differences between each component being very minor and hard to detect, a problem that is exacerbated by the presence of interference fringing or sloping baselines, both of which were common in the infrared spectra of the acrylic-based bicomponent fibers. Creslan 68 (American Cyanamid Co., Bound Brook, NJ) is an example of a fiber that is identified in a fiber reference library as being bicomponent (acrylic/acrylic), but in which the two components may be so chemically similar that spectroscopic differences are either undetectable or masked by interference fringing.

Another possibility is that the samples, although referred to as bicomponent samples, may indeed contain only one component. It was reported by Grieve et al. that the chemical composition of random bicomponent fibers, such as Acrilan B94 (Monsanto), Creslan 68 (American Cyanamid Co.) and Beslon F040 (Toho Rayon), can vary through all possibilities from 100% of one polymer to 100% of the other polymer (6). Obviously the examination of fibers at the extremes of these composition ranges will be particularly difficult. It is possible that some of the random bicomponent samples examined in this study did contain close to 100% of one polymer, explaining why the spectrum of only one polymer was detected. It may also be possible that the size of the regions of one component may be too small to be spatially resolved by infrared chemical imaging. As mentioned previously, a spatial resolution of around 5.5–15 µm is possible with the "normal" field of view. Therefore, if regions of one component are smaller than the best spatial resolution possible, this component would either go undetected by infrared chemical imaging, or its spectra would be averaged with those of the other component. The composition of the polymers contained in the fibers were still able to be determined using the infrared spectra obtained, and by following the classification schemes previously mentioned (see Table 1).

Cross-sectional analysis of the fibers was fairly tedious and time-consuming. Unfortunately, the majority of commercially available embedding resins are purposely designed to be colorless, to allow for the correct orientation of samples within the resin, and for microtoming. It was therefore necessary to dye the resin material to overcome the initial difficulties in locating the

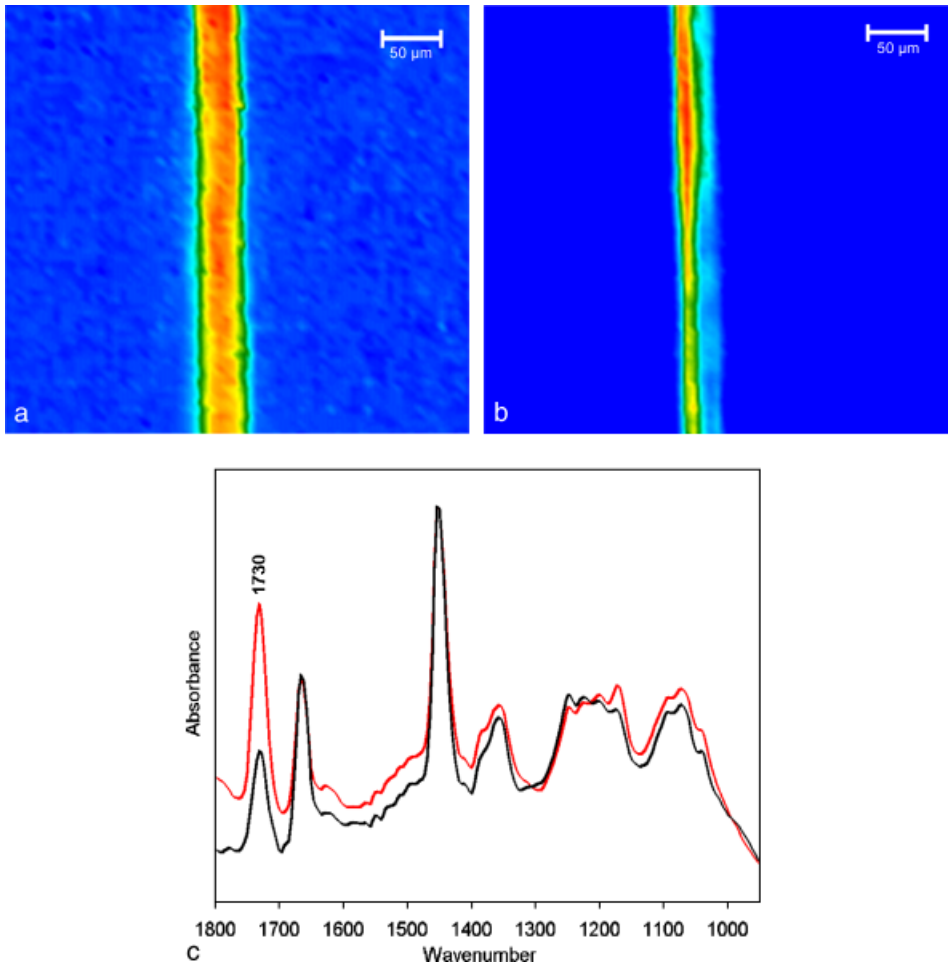

FIG. 8—*Infrared chemical image of Dralon K (Bayer) formed by imaging using the peak area at (a) 2244 cm^{-1} and (b) 1732 cm^{-1}. (c) Infrared spectra of the two components in Dralon K (Bayer), with the increased peak intensity indicated at 1730 cm^{-1}.*

white-to-colorless fibers in the colorless resins. Once the resins were dyed purple, it was a much simpler task locating the fiber cross-sections for imaging. Excellent results were obtained for Monvelle (Monsanto), with the two side-by-side components clearly visible in the infrared chemical image of the fiber cross-section (Fig. 10). Unfortunately, the resins appeared to infiltrate the rest of the fiber samples (most of which were acrylic-based) and no remedy for this was found in this study. However, cross-sectional analysis of possible bicomponent fibers using infrared chemical imaging would be the ideal approach where possible and convenient, as it would remove the ambiguities inherent to side-on analysis, particularly for sheath–core fibers and would overcome the occasional problems (indicated above) caused by the flattening of side-by-side fibers.

Overall, infrared chemical imaging was shown to be a technique that can provide spatially resolved chemical information on bicomponent fibers as long as detectable spectral differences exist between the two components. The common conventional techniques were shown to occasionally detect and spatially characterize side-by-side bicomponent fibers; however, unlike infrared chemical imaging, such techniques fail to provide chemical information on the components present. Unfortunately, no one technique examined was shown to work for all of the types of bicomponent fibers analyzed in this research. Although infrared chemical imaging will not identify/analyze bicomponent fibers with success in all cases, it does improve significantly upon the standard methods of analysis, and would be an asset when used in conjunction with these.

Conclusion

In summary, infrared chemical imaging has been demonstrated as a technique that can be used to both recognize and provide spatially resolved chemical information for those bicomponent fibers where it is possible to detect spectral differences between the two components present. It is a relatively rapid technique (5–6 min for 256 scans at 8 cm^{-1} resolution) that provides a large wealth of information, which includes not only the spectral signatures of the chemical components of a sample, but also their locations within the sample. As demonstrated, results can be visualized in numerous different ways, including the forming of chemical images, which allow the spatial distribution of the two components in the fiber sample to be clearly seen, an obvious advantage for displaying results to a layperson such as a jury member. While it was not successful in providing spatial information for certain samples examined in this research (where the two components were chemically very similar), the potential of infrared chemical imaging has clearly been demonstrated, with its ability to reveal both a fiber's chemical composition and spatial configuration with a single measurement. Few other techniques (apart from perhaps Raman chemical imaging) would be capable of providing this information without any prior knowledge of the

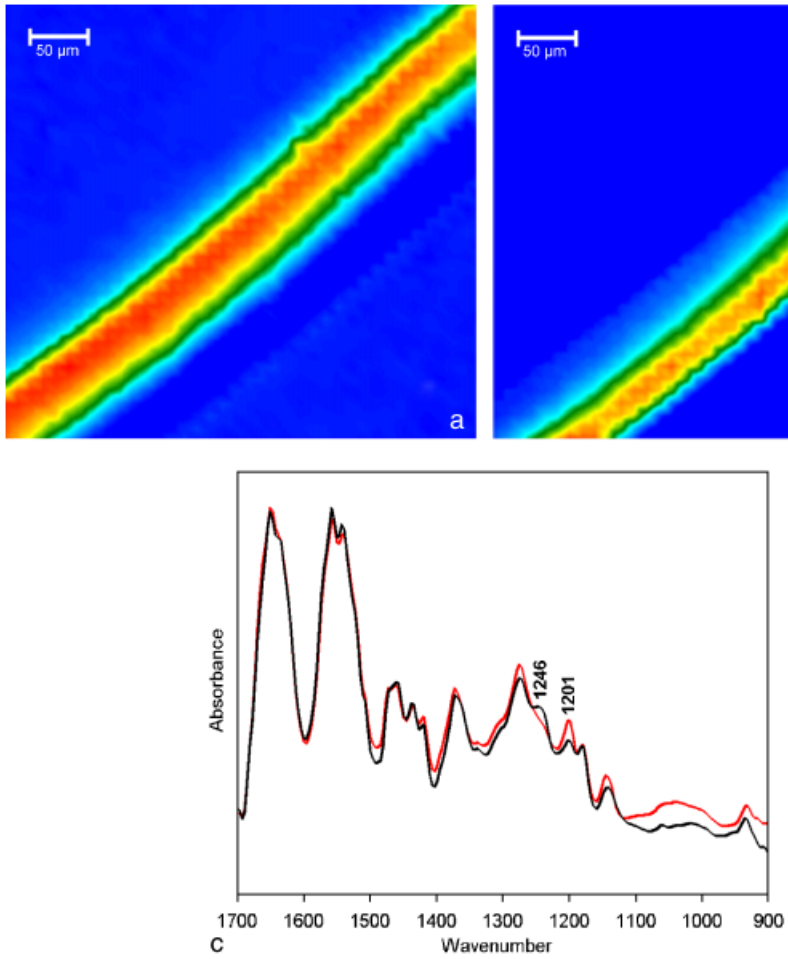

FIG. 9—*Infrared chemical image of Cantrece (DuPont) formed by imaging using the peak area at (a) 1246 cm^{-1} and (b) 1201 cm^{-1}. (c) Infrared spectra of the two components in Cantrece (DuPont).*

fiber's bicomponent nature and the configuration of its components, although more research is required before introducing this method into a routine case-working environment. When the method reaches its potential, the case-working analyst will require advanced skills to conduct the imaging and spectral interpretation.

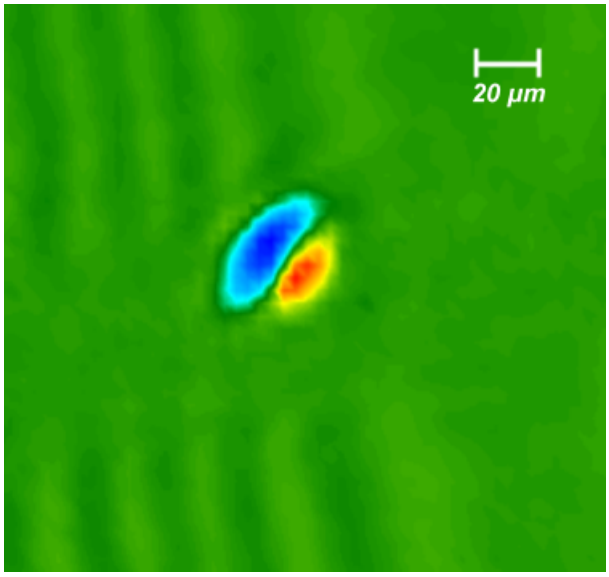

FIG. 10—*Infrared chemical image (1648 cm^{-1}) of a fiber cross-section from Monvelle (Monsanto).*

It should be noted that only integrated peak intensities were used here to attempt imaging of fibers. Multivariate statistical techniques such as hierarchical cluster analysis (HCA) can be used to highlight small but consistent differences between spectra (10). Alternatively, composite images based on spectral intensities at more than one wavelength can be constructed. Such techniques could be employed in the analysis of bicomponent fibers, but would require even higher levels of operator expertise.

As recent patents report the use of materials such as polyethylene, polyester, and nylon to produce bicomponent fibers (18), and as the use of bicomponent fibers is expected to increase in the future, infrared chemical imaging should grow in importance as a forensic tool for the detection and identification of such fibers where there is a measurable spectral difference between the two components.

Acknowledgments

The authors would like to thank Ms. Katie McBean for assistance with electron microscopy and David Royds (Australian Federal Police) for providing fiber samples. Thanks also goes to Dr. Ed Bartick (FBI) for access to bicomponent fiber infrared libraries. We would like to acknowledge funding for the infrared chemical imaging facility, as well as for the other instruments used in

this study, from the Australian Research Council's Linkage Infrastructure Equipment and Facilities scheme and collaborating institutions. K. F. gratefully acknowledges receipt of an Australian Postgraduate Award scholarship.

References

1. Kirkbride KP, Tungol MW. Infrared microspectroscopy of fibres. In: Robertson J, Grieve M, editors. Forensic examination of fibres. Philadelphia: Taylor & Francis; 1999:179–222.
2. Zapletalova T. Introduction to bicomponent fibers. Int Fiber J 1998;13:20–4.
3. http://www.fibersource.com [last accessed 28th January 2005].
4. Miller H. Keeping FIT with bicomponents: cha's fiber innovation technology fills niche in specialty fibers. Int Fiber J 1998;13:44–7.
5. Thoennessen F, Dahringer J. Trevira bicomponent fibers for nonwovens. Chem Fibers Int 2003;53:422–5.
6. Grieve MC, Dunlop J, Kotowski TM. Bicomponent acrylic fibers—their characterization in the forensic science laboratory. J Forensic Sci Soc 1988;28:25–33.
7. Tungol MW, Bartick EG, Montaser A. Analysis of single polymer fibres by fourier transform infrared microscopy: the results of case studies. J Forensic Sci 1991;36:1027–43.
8. Cho L, Reffner JA, Gatewood BM, Wetzel DL. Single fiber analysis by internal reflection infrared microspectroscopy. J Forensic Sci 2001;46:1309–14.
9. Tahtouh M, Kalman J, Roux C, Lennard C, Reedy B. The detection and enhancement of latent fingermarks using infrared chemical imaging. J Forensic Sci 2005;50:64–72.
10. Flynn K, O'Leary R, Lennard C, Roux C, Reedy BJ. Forensic applications of infrared chemical imaging: multi-layered paint chips. J Forensic Sci 2005;50:832–41.
11. Koenig JL, Wang S-Q, Bhargava R. FTIR images. Anal Chem 2001;73:360A–9A.
12. Nelson WG, Woods JL. An effective method for mounting fibres to allow simple processing, embedding and alignment for sectioning. J Microsc 1996;181:88–90.
13. Miyakawa M. Method for removing interference spectra in FT-IR microspectroscopy. Bunseki Kagaku 1994;43:57–60.
14. Sommer AJ, Tisinger LG, Marcott C, Story GM. Attenuated total internal reflection infrared mapping microspectroscopy using an imaging microscope. Appl Spectrosc 2001;55:252–6.
15. Chan KLA, Kazarian SG. New opportunities in micro- and macro-attenuated total reflection infrared spectroscopic imaging: spatial resolution and sampling versatility. Appl Spectrosc 2003;57:381–9.
16. Grieve MC. Another look at the classification of acrylic fibres, using FTIR microscopy. Sci Justice 1995;35:179–90.
17. Yang JC, Jablonsky MJ, Mays JW. NMR and FT-IR studies of sulfonated styrene-based homopolymers and copolymers. Polymer 2002;43:5125–32.
18. Kihara Y, inventor. Unitika Ltd. Nonwoven fabric made of core/sheath type composite fiber and process for producing the same. European Patent WO2004035900, 2004.

Additional information and reprint requests:
Brian J. Reedy, Ph.D.
Department of Chemistry, Materials and Forensic Science
University of Technology
Sydney
PO Box 123
Broadway NSW 2007
Australia
E-mail: Brian.Reedy@uts.edu.au